JCTC Journal of Chemical Theory and Computation

Article

pubs.acs.org/JCTC

Performance of Non-Local and Atom-Pairwise Dispersion Corrections to DFT for Structural Parameters of Molecules with Noncovalent Interactions

Waldemar Hujo[†] and Stefan Grimme*[,‡]

[†]Theoretische Organische Chemie, Organisch-Chemisches Institut der Universität Münster, Corrensstr. 40, D-48149 Münster, Germany

[‡]Mulliken Center for Theoretical Chemistry, Institut für Physikalische und Theoretische Chemie der Universität Bonn, Beringstr. 4, D-53115 Bonn, Germany

Supporting Information

ABSTRACT: The nonlocal, electron density dependent dispersion correction of Vydrov and Van Voorhis (Vydrov, O. A.; Van Voorhis, T. *J. Chem. Phys.* **2010**, *133*, 244103), termed VV10 or DFT-NL, has been implemented for structural optimizations of molecules. It is tested in combination with the four (hybrid)GGA density functionals TPSS, TPSS0, B3LYP, and revPBE38 for *inter*- and *intra*molecular noncovalent interactions (NCI) and compared to results from atom-pairwise dispersion corrected DFT-D3. The methods are applied to a wide range of different problems, namely the S22 and S66 test sets, large transition metal complexes, water hexamer clusters, hexahelicene, and four other difficult cases of intramolecular NCI. Critical interatomic distances are computed remarkably accurately by both dispersion corrections compared to theoretical or experimental reference data and inter- and intramolecular interactions are treated on equal footing. The methods can be recommended as reliable and robust tools for geometry optimizations of large systems in which long-range dispersion forces are crucial.

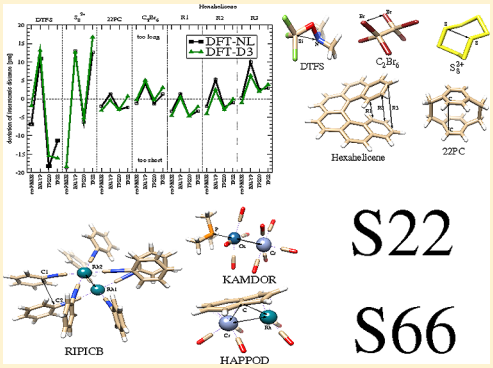

INTRODUCTION

Kohn−Sham Density Functional Theory (DFT) corrected for London dispersion[1,2] interactions is an ongoing success story that has lasted for some years. Dispersion interactions are omnipresent in chemistry and biology,[3] and therefore it is of fundamental importance to incorporate them in a physically sound manner into standard functional approximations. Most current dispersion corrections[4] use atom pairwise additive schemes,[5] but extensive density functional parametrization,[6] effective one-electron potentials,[7] or mixed density-based/atom pairwise schemes are also applied[8−11] to fix the problem. The nonlocal dispersion density functionals vdW-DF2[12] and VV10[13] use the electronic charge-density as the only input and incorporate the physics of dispersion-type correlation effects in a seamless manner. Recently, the excellent performance of the nonlocal (NL) VV10 dispersion correction for energetic properties was demonstrared for noncovalent interactions (NCI)[14−16] and thermochemistry[17] in combination with gradient corrected and global hybrid density functionals.

Previous assessments of the accuracy of DFT-NL for structural parameters were performed by means of potential energy curves[13,16] for dispersion dominated and mixed complexes (electrostatic/dispersion). Recently, we applied the rPW86-PBE-NL functional to weak hydrogen bonds.[14] We computed potential energy curves and found a slight shortening of the equilibrium distances compared to coupled-cluster reference curves with an error range of −2 to −10 pm. For cation−anion aggregates representing ionic liquids[15] B3LYP-NL and revPBE38-NL yielded slightly shorter equilibrium distances by up to −2 pm compared to reference CCSD(T)/CBS data. While these results are very encouraging, however, a more systematic investigation of DFT-NL for geometrical parameters of a diverse set of molecules and complexes has not been performed so far.

This work aims to answer the question of how well the nonlocal dispersion correction VV10 can describe structural parameters of molecules and their complexes. The S66 and S22 sets for general *inter*molecular NCI, water cluster hexamers, transition metal complexes, and difficult *intra*molecular cases are used to test the methods. The results are compared to those from the well-established DFT-D3 method[5,18] employing the same density functionals. Because both types of dispersion corrections have a negligible effect on "normal" (covalent) bond lengths,[13,18] only inter- as well as intramolecular NCI cases are considered here. Note that the tested dispersion corrected DFT methods have been extensively investigated in the past not only for the interaction energies of noncovalently

Received: September 17, 2012
Published: October 26, 2012

bound complexes[4,5,13−20] but also for thermochemical properties of molecules.[17,20] In general, very good accuracy for NCI energies with typical relative errors of 5−10% are obtained for both, DFT-NL and DFT-D3. Because this has been repeatedly published by other groups (see e.g. ref 21), we concentrate in this work on the performance for computing structures and refer the reader to the literature for a detailed discussion of the performance for interaction energies. We will first present our methodological approaches, the systems under investigation, and computational details, followed by the key results with discussion and final conclusions.

METHODOLOGY

We compute the structural parameters by relaxation of the molecular geometry using unconstrained energy minimization (nonlinear optimization) calculations in combination with meta-(hybrid)GGA density functionals using a quasi-Newton−Raphson scheme (see Computational Details). Opposed to a potential energy minimum scan along a well-defined coordinate of (usually) only one dimension, a full geometry optimization yields a potential energy minimum on a $3N - 6$ dimensional potential surface and is therefore in general more meaningful for a benchmark.

For intermolecular interactions we use the popular benchmark sets S22[22] and S66,[23] which contain a broad range of different kinds of molecules with NCI encompassing hydrogen bonds, van der Waals complexes, and molecules with a mixture of both types of interactions. In particular, the recently designed S66 set improves on S22 by a larger number of molecules, which are additionally more balanced in terms of chemical diversity. However, completely optimized CCSD(T)/CBS reference structures for these sets are not available. Therefore, we take as reference intermolecular separations of CCSD(T)/CBS quality with the original monomer geometries optimized at the MP2/triple-ζ level. We used the CCSD(T)/CBS energies of the S22x5[24] set to construct dissociation curves and to obtain a new minimum of the intermolecular separation at the coupled cluster level. We interpolated the five points per molecule with spline functions and took the resulting minimum as a reference. We term this new set of reference structures as "S22d". For the S66 set, we take the geometries provided by the authors in ref 23. These were obtained by using intermonomer potential energy minimum geometries of CCSD(T)/CBS calculations and dubbed the S66x8 set (similar to the protocol for S22x5 above). The possible differences and pitfalls when comparing such estimated equilibrium structures to those from full optimizations are discussed below.

To estimate the accuracy of the DFT structural optimizations, we use as measures the center of mass (CM) and hydrogen-bond (HB) distances. The CM distance is the length of the vector from the center of mass of one molecule to the center of mass of the other molecule in the complex. A HB consists of the fragments X−H···Y−Z, where X−H is the proton-donating group and Y−Z is the proton-acceptor group. We use the HB distance R(H···Y) as an additional parameter.

As an example for a hydrogen-bond network-building system, we consider the smallest water cluster that forms a three-dimensional structure which is the water hexamer. The clusters named "cage," "prism," and "book" were recently confirmed theoretically and experimentally by Pérez[25] and co-workers to be the three low-energy isomers in the mentioned order. The experimental hydrogen framework structures were identified by means of oxygen positions in the cluster, and a best estimate for the gas phase was computed at the MP2 level.

Additionally, we compiled a diverse set of five molecules (see Figure 1) with intramolecular noncovalent interactions, which

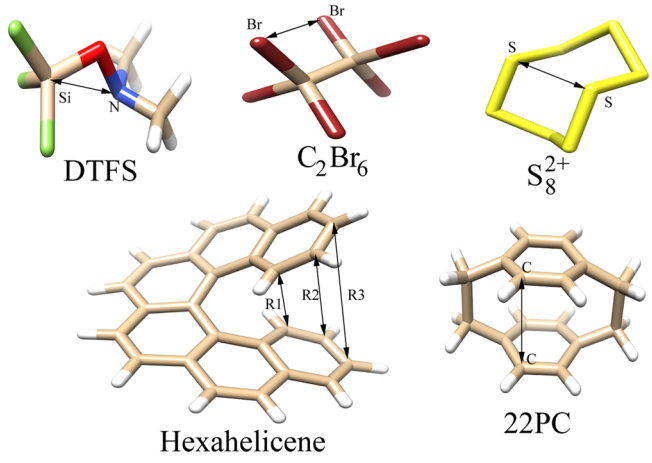

Figure 1. The molecules (N,N-dimethylaminoxy)trifluorosilane (DTFS), hexabromoethane (C_2Br_6), cyclooctasulfur dication (S_8^{2+}), and [2,2]paracyclophane (22PC) represent four difficult cases with noncovalent intramolecular interactions. The hexahelicene molecule serves as an example for sterically overcrowded polycyclic aromatic hydrocarbons.

are difficult for dispersion uncorrected density functionals.[18] These are (N,N-dimethylaminoxy)trifluorosilane (DTFS),[26] cyclooctasulfur dication (S_8^{2+}),[27] [2,2]paracyclophane (22PC),[28] and hexabromoethane (C_2Br_8).[29] As an example for polycyclic aromatic hydrocarbons (PAH) and carbon-rich materials, we enclose the hexahelicene[30,31] molecule. It is composed of six benzene rings, which are connected in ortho positions to each other. The distinctive property of helicenes is their helical (chiral) structure (for a recent review see ref 31) which results from a detailed interplay of Pauli-exchange repulsion and dispersion attraction. The reference values for the gas-phase structure were estimated from the experimental X-ray[30] data and correcting for the difference of molecular revPBE-D3 and periodic revPBE-D3 calculations[32] (i.e., excluding packing effects).

We also included three example molecules containing early and late transition metals (see Figure 2). The first is the isonitril

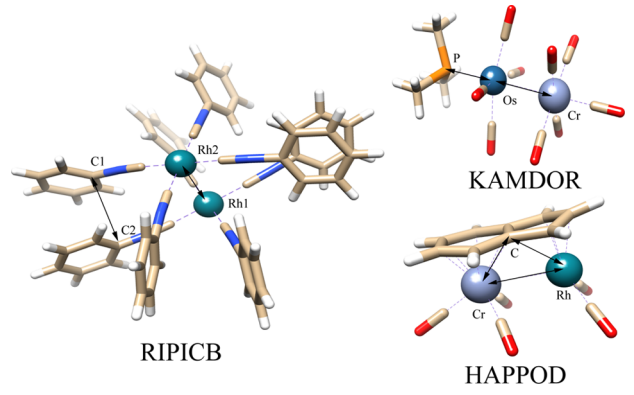

Figure 2. The systems RIPICB, KAMDOR, and HAPPOD considered as examples for transition metals complexes with intramolecular noncovalent interactions.

dx.doi.org/10.1021/ct300813c | J. Chem. Theory Comput. 2013, 9, 308−315

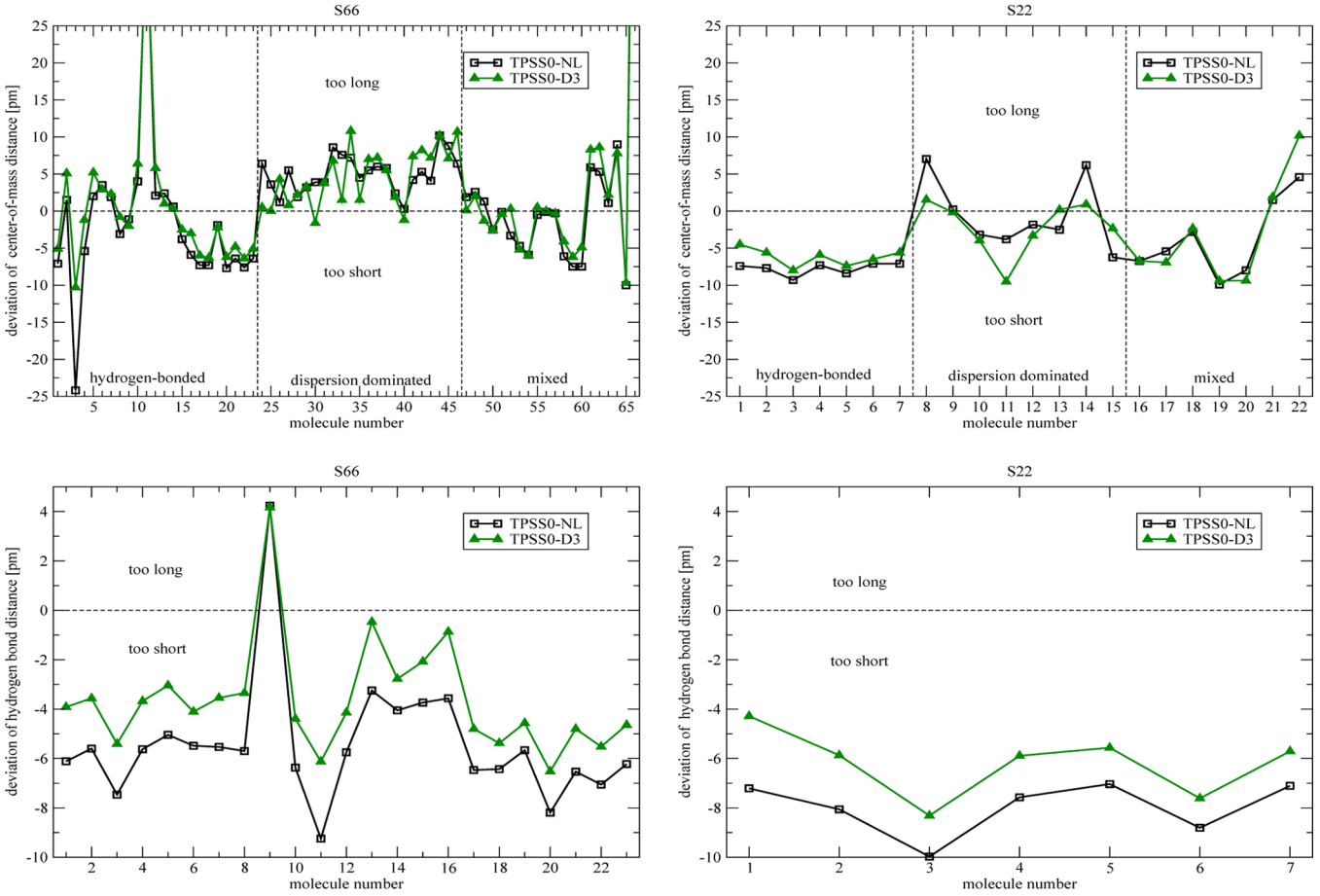

Figure 3. The upper two graphs show deviations of center-of-mass distances in pm for the S66 and S22d noncovalent interaction benchmark sets. The lower two graphs show deviations for the hydrogen bond lengths in S66 and S22d subsets only.

rhodium(I) bis-cation dimer[33] $[(PhCN)_4Rh]_2^{2+}$, which has the reference code RIPICB in the Cambridge Structural Database. In a recent study[34] in our laboratory, we showed that the attractive dispersion forces mainly between the substituents can overcome the overwhelming Coulombic repulsion of the metallic core, which explains the stability of such charged complexes. In the second and third examples, we concentrate on metallophilic interactions within the closed-shell $(CH_3)_3P$-$(CO)_4Os\cdots Cr(CO)_5$[35] molecule (with the reference code KAMDOR) and the syn-$[Cr(CO)_3$-indenyl-$Rh(CO)_2]$ complex (with reference code HAPPOD). The nature of the Os···Cr and Rh···Cr interactions was shown[36,37] to be dominated by dispersion forces as well.

In our study, we enhance the meta-GGA density functional TPSS,[38] the global hybrid meta-GGA TPSS0,[39] and the global hybrids B3LYP[40,41] and revPBE38[5,20,42−44] with the atom-pairwise and nonlocal dispersion corrections. The TPSS and TPSS0 density functionals were chosen due to their good performance for geometry parameters in combination with the D3 dispersion correction. B3LYP was chosen, because it is widely used and showed recently very good performance with the VV10 dispersion correction.[17] We also consider the hybrid density functional revPBE38, which contains the largest admixture of Fock-exchange (E_x^{HF}) of 37.5% (3/8), compared to B3LYP with 20% and TPSS0 with 25%. The density functionals were not modified specifically in order to preserve comparability with previous (dispersion uncorrected) investigations and between both dispersion corrections. Although this selection is not extensive, we nevertheless think that general conclusions regarding the applicability of the tested dispersion corrections can be drawn from our study.

The total exchange-correlation E_{xc}^{DFT-NL} energy of the DFT-NL method consists of the standard DFT exchange and short-range correlation part E_{xc}^{DFT} and the nonlocal (mainly long-range) dispersion correction E_{c-NL}^{VV10} according to

$$E_{xc}^{DFT-NL} = E_{xc}^{DFT} + E_{c-NL}^{VV10} \quad (1)$$

The Cartesian energy gradient of the total exchange-correlation energy of DFT-NL with respect to displacements of atom A is defined as a sum of the standard DFT gradient and the nonlocal gradient

$$\nabla_A E_{xc}^{DFT-NL} = \nabla_A E_{xc}^{DFT} + \nabla_A E_{c-NL}^{VV10} \quad (2)$$

where the last term is given by

$$\nabla_A E_{c-NL}^{VV10} = g_{GBF}^A + g_{weights}^A + g_{grid}^A \quad (3)$$

with contributions of the Gaussian basis set (g_{GBF}^A), the derivatives of the numerical quadrature weights ($g_{weights}^A$), and the explicit dependence of the intergrid distance of the grid points (g_{grid}^A). The definitions of the nonlocal energy term E_{c-NL}^{VV10} and the three gradient terms g_{GBF}^A, $g_{weights}^A$, and g_{grid}^A are given by Vydrov and Van Voorhis in ref 13. The nonlocal dispersion correction E_{c-NL}^{VV10} contains the empirical short-range attenuation parameter b, which was fitted to energies in the S22 set for the functionals B3LYP (b = 4.8) and revPBE38 (b = 4.7) as

Table 1. The Mean Absolute Deviation (MAD) and Mean Deviation (MD) in pm from Center-of-Mass Distances for the S66 and S22d Noncovalent Interaction Benchmark Sets with Non-Local (NL) and Atom-Pairwise Dispersion Correction (D3)[a]

	S66				S22d			
	MAD		MD		MAD		MD	
	NL	D3	NL	D3	NL	D3	NL	D3
revPBE38	7 (1)	3 (1)	4 (−1)	−1 (0)	5 (2)	5 (1)	−2 (−2)	−5 (−1)
B3LYP	7 (1)	3 (1)	4 (−1)	0 (−1)	4 (2)	4 (1)	−2 (−2)	−3 (−1)
TPSS0	6 (2)	6 (1)	2 (−2)	3 (−1)	6 (3)	5 (2)	−4 (−3)	−4 (−2)
TPSS	7 (4)	9 (2)	3 (−1)	7 (−2)	5 (3)	5 (2)	−4 (−3)	0 (−2)

[a]The deviations of the hydrogen bond distances for the corresponding seven molecules in the S22d set and the 23 molecules in the S66 set are given in parentheses.

reported previously.[17] In the present work, we used the S66 set analogously to obtain the optimal values $b = 5.0$ for TPSS and $b = 5.5$ for TPSS0.

The atom-pairwise dispersion correction DFT-D3 is the simplest way of providing an asymptotically correct R^{-6} dependence of the dispersion energy on the intermolecular distance R. Opposed to vdW-DFs, the method provides a nonelectronic dispersion energy without any significant additional computational cost. Recently, we extended the DFT-D3[5] approach with the Becke and Johnson (BJ) rational damping function,[8,45,46] for which the analytical Cartesian gradient is readily available, such that efficient geometry optimizations can be performed. In the following, we use the term "DFT-D3" as a synonym for "DFT-D3(BJ)", which is our default for DFT-D3 calculations. In some cases, we compare with older dispersion variants, such as the D3(zero)[5] and D2[47] versions.

COMPUTATIONAL DETAILS

All DFT calculations were carried out with a locally modified version of the Turbomole[48] suite of programs. The DFT-NL Cartesian gradient can be readily obtained if the NL electronic potential is self-consistently included in the DFT calculation. In passing, it is noted that this is usually not required for interaction energy calculations for which the effect of an SCF-NL treatment is negligible.[15] We compared our implementation of the analytical NL gradient carefully with the numerical one and found excellent agreement. The computations employ the resolution of the identity method (RI)[49,50] for electronic Coulomb energy and the large def2-QZVP[51] AO basis set which provides results close to the basis set limit.[20,52] Basis set superposition errors are negligible for (hybrid)GGA computations with such large basis sets,[47] and consequently, counterpoise corrections are not applied. For the systems RIPICB, KAMDOR, and HAPPOD, we employed the def2-TZVP[53] basis set along with standard (large core) effective potentials.[54] For the numerical quadrature, we choose the so-called *m4* grid for the exchange-correlation and NL parts. All calculations were performed in gas phase and without any symmetry constraints in the C_1 point group. The thresholds for the energy convergence of 5×10^{-7} atomic units and for the RMS norm of the Cartesian gradient change of 5×10^{-5} atomic units was used. We employ the quasi-Newton−Raphson geometry optimization method, where for the Hessian matrix update procedure the variant of BFGS (Broyden−Fletcher−Goldfarb−Shanno) was applied as implemented in the program statpt of the Turbomole[48] package.

RESULTS AND DISCUSSION

First, we present the equilibrium intermolecular distances of the S22d and S66 sets (see Figure 3 and Table 1), the three water hexamer clusters (Table 2), and the transition metal complexes

Table 2. The Averaged Shortest Oxygen−Oxygen Distances in the Cage (8), Prism (9), and Book (7) Structures, Resulting in a Characteristic Mean Value $\bar{R}$(O···O) in pm for Each Cluster Isomer

	cage		prism		book	
	$\bar{R}$(O···O)		$\bar{R}$(O···O)		$\bar{R}$(O···O)	
	NL	D3	NL	D3	NL	D3
revPBE38	279	281	282	284	274	276
B3LYP	277	280	280	283	273	275
TPSS0	275	278	278	281	272	273
TPSS	274	277	277	281	271	273
MP2(best est.)[25]	281		284		277	
exptl[25]	285		289		280	

(Table 3 shown also in Figure 2). Second, we will discuss the investigated intramolecular distances (Table 4 and Table 5) of the systems depicted in Figure 1.

S66 and S22d Sets. From the four investigated NL and D3 dispersion corrected density functionals in this study, the most balanced results for the S66 and S22d sets were found with TPSS0. Comparing the deviations of the center of mass (CM) distances of TPSS0 for the entire sets, our calculations yield for S66 and S22d mean absolute devations (MADs) (mean deviation, MD, in parentheses) of 6 (2) and 6 (−4) pm for the NL correction and 6 (3) and 5 (−4) pm for the D3 correction, respectively. Similar high accuracy is obtained for the hydrogen bond distances (HB) of the S66 and S22d sets with MAD (MD) values of 2 (−2) and 3 (−3) pm for NL and 1 (−1) and 2 (−2) pm for D3 (see Table 1)

With the NL dispersion correction, the best performance for the S66 set was found in combination with TPSS0 and for S22d with B3LYP, which partially may result from the used fit sets; i.e., TPSS0 was fitted to interaction energies of the S66 set and B3LYP to the S22 set. For the D3 dispersion correction, the B3LYP functional performs best for both the S66 and S22d sets. For both sets, the best overall results were gained by the B3LYP-D3 method with an MAD (MD) for the S66 set of 3 (0) pm and for the S22d set of 4 (−3) pm for the CM distances.

Neglecting dispersion corrections makes bare density functionals in practice unusable for the structural chemistry of NCI. For the S66 set, uncorrected density functionals yield MADs from 97 pm (TPSS0) to 172 pm (B3LYP) and for the

dx.doi.org/10.1021/ct300813c | J. Chem. Theory Comput. 2013, 9, 308−315

Table 3. Interatomic Distances for Transition Metal Complexes with Dispersion Corrected DFT[a]

	KAMDOR				HAPPOD						RIPICB			
	R(Os···Cr)		*R*(Os···P)		*R*(Rh···Cr)		*R*(C_b···Cr)		*R*(C_b···Rh)		*R*(Rh···Rh)		*R*(C···C)	
	NL	D3	NL	D3	NL	D3	NL	D3	NL	D3	NL	D3	NL	D3
revPBE38	298	315	233	233	305	306	235	236	255	256				
B3LYP	306	314	237	237	314	316	241	243	262	263				
TPSS0	296	297	233	234	302	304	235	236	255	255				
TPSS	294	298	235	236	301	304	236	237	257	258	299	304	375	375
X-ray[36,37]	298		235		308		240		254		319		358	

[a]The molecules KAMDOR, HAPPOD, and RIPICB are depicted in Figure 2. All distances are given in pm. Here, C_b denotes the bridged carbon atom in HAPPOD.

Table 4. Interatomic Distances of (N,N-Dimethylaminoxy)trifluorosilane (DTFS), Hexabromoethane (C_2B_{68}), Cyclooctasulfur Dication (S_8^{2+}), and [2,2]Paracyclophane (22PC) in pm

	DTFS		S_8^{2+}		22PC		C_2Br_6	
	R(Si···N)		*R*(S···S)		*R*(C···C)		*R*(Br···Br)	
	NL	D3	NL	D3	NL	D3	NL	D3
revPBE38	220	225	267	268	308	306	341	342
B3LYP	238	240	299	299	311	309	346	347
TPSS0	209	212	280	281	307	307	341	342
TPSS	216	211	299	303	307	310	343	345
exptl	227[26]		286[27]		310[28]		342[29]	

Table 5. Carbon−Carbon Distances in the Hexahelicene Molecule in pm[a]

	R1(C···C)		R2(C···C)		R3(C···C)	
	NL	D3	NL	D3	NL	D3
revPBE38	306	305	417	415	514	512
B3LYP	311	310	424	422	523	520
TPSS0	305	305	417	416	516	515
TPSS	306	307	418	419	516	517
gas-phase, est. exptl.[32,59]	309		418		516	
corr. solid−gas	13		40		47	
X-ray[30]	322		458		563	

[a]The distances R1, R2, and R3 are defined in Figure 1. The corrections from the gas phase to the solid state are also given.

S22d set MAD values from 64 pm (TPSS0) to 118 pm (B3LYP). The more strongly repulsive potential of B3LYP yields much too long distances, such that many complexes hardly exhibit any interaction in the final, optimized structure. However, for hydrogen bonds, uncorrected TPSS shows comparable performance to its dispersion corrected pendant, due to its rather attractive potential in the medium-range correlation regime (see the Supporting Information).

In the following, we will have a closer look at the dispersion corrected TPSS0 results (see Figure 3). It is remarkable to note that in all four figures the TPSS0-D3 and TPSS0-NL error curves are very close to each other, and the error pattern is very similar. For the seven hydrogen bonded systems in the S22d set (i.e., entries 1−7), it is worth mentioning that the CM errors (in the upper panel) and the errors for the HB distances (in the lower panel) are similar, and the error curves have a similar shape. This suggests that the monomers in the hydrogen bonded systems do not alter significantly their positions relative to each other, meaning that geometrical displacements and rotations affect both types of distances equally (CM and HB). However, the patterns for the 23 hydrogen bonded systems of the S66 set regarding the CM and HB errors look somewhat differently. This suggests that the full geometry optimization has more altered the structure of the entire complex. However, except for a few outliers in the S66 set, the deviations are small and not alarming.

Four outliers were found for TPSS0-NL and three for TPSS0-D3 (Figure 3). Systems 11 and 66 yield very large CM distances as well as system 9 for the HB distance. Additionally, system 3 yields a large error for TPSS0-NL. These outliers were also found for the other NL/D3 corrected functionals except for B3LYP-NL, which shows a reasonable HB distance for system 9. Also revPBE38-D3 and B3LYP-D3 yield a proper CM distance for system 66. The S22d set, on the other hand, produced no outliers. The question of whether these systems should be considered DFT failures or if very flat potential energy surfaces together with incompletely optimized MP2 reference geometries cause the observed substantial differences cannot be answered at present. The only hydrogen bonded system whose HB distance is elongated and not shortened as in the other systems is $MeNH_2$···MeOH (system 9). With the exception of B3LYP-NL, all dispersion corrected density functionals investigated in this study show this deviation. Except for revPBE38-D3, essentially all other methods overbind hydrogen bonds (with the outlier system 9), resulting in too short bonding distances. The slight tendency of overbinding hydrogen bonds with the two dispersion corrections D3 and NL may be interpreted as some kind of correlation energy double-counting effect at medium distances (i.e., to the reasonable description of hydrogen bonds by the density functional a further attractive potential is added). This can easily be avoided by adjusting the standard density functional to the presence of the dispersion correction (as e.g. in B97d[47]) but is not considered in our work here.

Water Hexamer Clusters. Hydrogen bonds in water clusters represent strong NCIs and are essentially of the directional dipole−dipole type with a small, but non-negligible influence of dispersion. We computed the mean of all shortest O···O distances in a cluster, resulting in a characteristic $\bar{R}$(O···O) value for each hexamer (Table 2). The DFT results are compared to those from relatively accurate MP2 calculations as well as experimental estimates.[25]

All dispersion corrected functionals yield slightly shorter bonds compared to the theoretically obtained gas-phase estimate.[25] For all clusters, revPBE38-D3 yields the most accurate $\bar{R}$(O···O) distances with deviations of −1 pm for book and exact mean distances for cage and prism, closely followed by B3LYP-D3. The best NL method is revPBE38-NL with deviations of −2 (cage, prism) and −3 pm (book). The

overbinding of hydrogen bonds is slightly more pronounced in hexamers than in the water dimer. The shortening of hydrogen bonds going from the dimer to the hexamer structure can be credited to cooperative binding effects within the cluster[55] by induction (polarization). This is probably overestimated by DFT, but a sligthly too flat short-range behavior of the dispersion-corrected exchange-correlation energy can also not be ruled out. Uncorrected revPBE38 and B3LYP yield too long $\bar{R}$(O···O) distances in the range of 1 to 5 pm. TPSS and TPSS0 yield mostly too short bonds in the range of −1 to −2 pm, except for prism, where TPSS0 yields a deviation of 11 pm.

Transition Metal Complexes. Previous theoretical studies on the KAMDOR molecule[36] (Table 3) with TPSS-D, B2PLYP-D,[56] and SCS-MP2[36] revealed shortening of the metal−metal R_e(Os···Cr) distance by −1, −7, and −16 pm, compared to the value for the crystal structure of R_0(Os···Cr) = 298 pm. In this study, revPBE38-NL and TPSS-D3 exactly reproduced the X-ray value for this parameter. For the R_e(Os···P) distance, the best agreement is found by TPSS-NL with a perfect match of the crystal structure value of 235 pm. Uncorrected DFs overestimate the metal−metal distance significantly by up to 22 pm (B3LYP) compared to the dispersion corrected result. For the metal−phosphorus bond, uncorrected DFs yield reasonable interatomic distances with exact agreement to the experimental value for revPBE38 and TPSS0 and a slightly too long distance for TPSS with 3 pm and B3LYP with 5 pm (see Supporting Information).

Previous computational investigations of HAPPOD with TPSS-D2 and SCS-MP2 provided[37] quite accurate Rh···Cr distances of 309 and 297 pm compared to the crystal structure value[57] of 308 pm. For the C_b···Cr distance (C_b is the bridged carbon atom), TPSS-D2 and SCS-MP2 both yield 237 pm, while for C_b···Rh the TPSS-D2 distance is, with 260 pm, quite long compared to the X-ray value of 254 pm. In our study, the most accurate Rh···Cr distance is obtained by revPBE38-D3 with 306 pm closely followed by revPBE38-NL with 305 pm. For the carbon−metal distances, the results for all dispersion corrected functionals are rather similar except for B3LYP, which yields too long distances. The dispersion corrected functionals revPBE38, TPSS0, and TPSS yield C_b···Cr values in a narrow range of 235 to 237 pm and for C_b···Rh in the range of 255 to 258 pm. Uncorrected TPSS (310 pm) and TPSS0 (309 pm) yield Cr···Rh distances quite close to the crystal structure value, where the other two DFs B3LYP and revPBE38 show longer metal−metal distances with 326 and 315 pm, respectively (see the Supporting Information).

In a recent study[34] in our group, a Rh···Rh distance of 311 pm in the RIPICB molecule (Figure 2) was computed at the TPSS-D3(zero)/def2-TZVP (COSMO) level of theory, which is somewhat shorter compared to the crystal structure distance of 319 pm. We have reinvestigated this system in the gas phase at the TPSS-NL and TPSS-D3 levels of theory with the same basis set and obtained Rh···Rh distances of 299 and 304 pm, respectively. For the C···C distance we found for both methods a value of R = 375 pm, which is somewhat longer compared with experimental results and the previous calculation (both 358 pm).

The overall best metal−metal distances for the transition metal complexes are computed by the NL corrected density functionals with a slight tendency to overbind.

Molecules with Intramolecular Noncovalent Interactions. The four systems DTFS, S_8^{2+}, 22PC, and C_2Br_6 (Figure 1) with quite short intramolecular distances were shown to be sensitive to the damping scheme applied in the D3 dispersion correction.[18] The Becke−Johnson rational damping[8] used here with the D3 dispersion correction yields a constant dispersion energy for very short interatomic distances as suggested by perturbation theory.[58] For the VV10 dispersion correction, a similar damping scheme is applied so that both methods are expected to yield a similar short-range behavior which is important in these intramolecular cases with typically shorter distances than for intermolecular complexes.

Previous gas phase electron-diffraction studies on (N,N-dimethylaminoxy)trifluorosilane (DTFS)[26] yield an Si···N distance of 227 pm which is much longer than in the crystal structure (196 pm). In the same study, gas-phase calculations at MP2/6-311G(d,p) and B3LYP/6-311+G(3df,3dp) levels of theory yielded too long distances of 229 and 244 pm, respectively. A recent theoretical study[18] at the PW6B95-D3(BJ) level gave a value of 212 pm. Here, we obtain the best value with revPBE38-D3 of 225 pm, closely followed by revPBE38-NL with 220 pm. Dispersion corrected methods based on TPSS underestimate the distance by −11 and −18 pm, while it is overestimated by B3LYP (11 and 13 pm). Density functionals without dispersion corrections yield distances in an error range of −5 (TPSS0) to 20 pm (B3LYP).

Together with DTFS, the cyclooctasulfur dication (S_8^{2+}) shows the shortest intramolecular distance investigated in this study and is most difficult to describe by DFT. Cameron et al.[27] measured a value of 286 pm for the critical S···S distance in the dication which is longer than typical covalent S−S bonds (about 200 pm) but much shorter than a typical S−S vdW interaction (about 360 pm). In that study, the authors computed at the B3PW91/6-311G(2df) level of theory a distance of 287 pm. In another study,[18] a very good distance of 285 pm was computed at the PW6B95-D3/def2-QZVP level. Here, the closest agreement between theory and experiment is obtained by TPSS-D3 and TPSS-NL with 281 and 280 pm, respectively. In ref 27, a Wiberg covalent bond index of 0.2 for the S···S interaction was computed, indicating only a small admixture of covalent binding. This might be a hint that the difficulties to describe this interaction are primarily rooted in the short-range correlation part of the density functionals, which cannot be compensated by dispersion corrections. Uncorrected DFT provides deviations in the range of −2 pm (TPSS0) to 25 pm (B3LYP) from the reference value.

The [2,2]paracyclophane (22PC) molecule was the subject of several experimental and theoretical studies (see ref 28 and references therein). The critical structural parameter is the interplanar distance of the two benzene rings, which experimentally is found to be 310 pm.[28] Previous theoretical studies at the SCS-MP2, PW6B95-D3, B3LYP-D3, and TPSS-D3 levels[18,28] provided distances of 308, 309, 309, and 310 pm, respectively. Our computations reveal an excellent result for B3LYP-NL of 311 pm. As already found for the previous two systems, uncorrected TPSS0 and B3LYP give the smallest and largest deviations from experimental results of 0 to 6 pm, respectively.

Mandel and Donohue[29] reported an intramolecular bromine−bromine contact of 342 pm in the hexabromoethane crystal. Computations at the PW6B95-D3 level of theory[18] yielded exactly this value. In our study, we also obtained the correct value with revPBE38-D3 and TPSS0-D3, closely followed by revPBE38-NL and TPSS0-NL, each providing rather accurate values of 341 and 343 pm for TPSS-NL. Similar

to 22PC, larger errors up to 7 pm (B3LYP) were computed for uncorrected functionals.

In conclusion, we found a low error range for 22PC and C_2Br_6 and somewhat larger deviations for DTFS and S_8^{2+} (Figure 4). In most cases, D3/NL dispersion corrected B3LYP

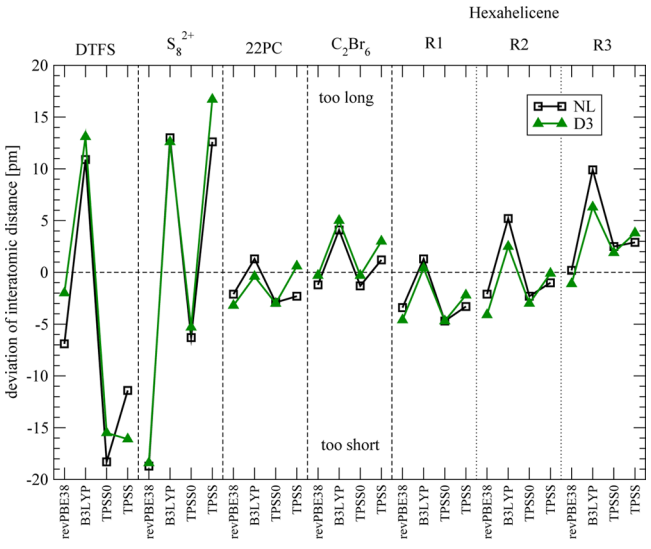

Figure 4. Deviations of interatomic distances in DTFS, S_8^{2+}, 22PC, and C_2Br_6 from experimental data in pm. For the hexahelicene molecule, a gas-phase estimate including theoretical corrections for packing effects has been used.

and TPSS overestimate the interatomic distances, while revPBE38 and TPSS0 underestimate them. The best results were obtained with revPBE38-D3/NL (37.5% Fock-exchange) and TPSS0-D3/NL (25%), which are comparable to the previous results at the PW6B95-D3 (28%) level,[18] indicating the importance of increased exact-exchange admixture. Uncorrected density functionals perform not too badly but are usually outperformed by the D3/NL variants.

Because the three molecules for which crystal structure data have been used for comparison are rather rigid, it is not expected that our conclusions are significantly affected by packing effects. This is not true in general and in particular does not hold for more flexible larger systems as investigated in our last example.

The hexahelicene molecule forms a single pitch that can be characterized by the three C···C distances from the most inner carbon atoms (R1, R2) to the outer carbon (R3) of the terminal benzene rings (see Figure 1). In a recent study, carried out in our group, periodic solid-state optimizations of hexahelicene at the revPBE-D3 level of theory were conducted and compared to the crystal structure data.[32] Very small deviations between theory and experimental results for the solid, e.g. of 3 pm for R3, were found. Gas-phase optimizations were carried out at the same level, which allowed an estimation of the structural deformation of the molecule in the solid-phase (Table 5) by packing effects. The computed gas-phase corrections as estimated from molecular and periodic revPBE-D3 calculations amount to 13, 40, and 47 pm for the pitches R1, R2, and R3, respectively.[59]

Our computations for the isolated molecule reveal slight shortening of the inner pitch distances and elongation of the outer pitch distances with respect to the estimated gas-phase data (Figure 4). From all density functionals tested, TPSS-NL provides the smallest errors of −3 pm for R1 and exact matches with the experimental gas-phase estimate for R1 and R3. Dispersion corrected B3LYP somewhat steps out of line compared to the other functionals by yielding too long pitches (by 4−7 pm for R2 and R3).

The uncorrected density functionals perform fortuitously well when isolated molecule computations are compared to raw crystal structure data. However, as pointed out in ref 32, this good agreement is based on error compensation. If large somewhat floopy molecules are considered, meaningfull comparisons should always be based on experimental results and theory for the same state (i.e., solid or gas). If uncorrected DFT is compared to the gas-phase estimate, large errors are found especially for R3 (e.g., up to 41 pm with B3LYP), while however, for R1 smaller deviations, of e.g. 3 pm for TPSS0, are obtained.

CONCLUSIONS

The atom-pairwise dispersion correction D3 as well as the nonlocal charge-density based dispersion correction VV10 (termed NL here) in combination with TPSS, TPSS0, B3LYP, and revPBE38 functionals yield simliar and accurate inter- and intramolecular distances for equilibrium structures of the S66 and S22d sets of noncovalent interactions, water hexamer clusters (cage, prism, and book), transition metal complexes (RIPICB, HAPPOD, and KAMDOR), hexahelicene, DTFS, S_8^{2+}, 22PC, and C_2Br_6.

For the intermolecular distances in the S22d and S66 sets, we obtained MADs (MDs) in the range of 3 (−5) to 9 (7) pm of the center of mass distances with D3 and NL. The B3LYP-D3 approach yielded overall the best performance. Both dispersion corrections result in slightly too short hydrogen bonds, where for DFT-NL this effect is more pronounced. The averaged $\bar{R}$(O···O) distances of the three low-energy water hexamer clusters were reproduced very well with an error range of −7 to 0 pm, where revPBE38-D3 gave the most accurate values for all three isomers. Transition metal complexes were assessed with the DFT-NL method for the first time in this work. The metal−metal distances were reproduced very well with all dispersion corrected methods compared to experimental data. Here, the NL corrected density functionals performed slightly better than those with the D3 correction. Intramolecular interactions were very well described with revPBE38 (and B3LYP), where both dispersion corrections provided similar results with somewhat better performance of D3. For all methods, the deviations of the distances from reference values varied between −19 and 17 pm with the largest problems for the S_8^{2+} system.

The atom-pairwise dispersion correction DFT-D3 overall provides the better accuracy-to-computational-cost ratio, due to its very good general performance and negligible computational overhead in DFT computations. The nonlocal dispersion correction DFT-NL provides very similar accuracy, however, at considerably higher computational and numerical complexity with a computation time overhead of at least 50% for the self-consistent and gradient calculations. The qualitative differences of these two dispersion corrections are rooted in the fact that the D3 correction yields more accurate molecular dispersion coefficients with a mean relative deviation[5] of 5%, where NL yields an error[13] of 9%. Although the D3 method contains precomputed C_6 dispersion coefficients based on accurate first-principles (TDDFT) calculations, it comprises high flexibility due to a dependence on the structure of a molecule (coordination numbers). Furthermore, the D3 corrected

density functionals gain more accuracy through inclusion of the higher-order multipole term R^{-8}. Opposed to NL, however, the D3 correction does not incorporate any electronic effects, which is not crucial for geometrical parameters, as has been shown in this study. Yet, based on the present results and our recent experience, DFT-NL offers advantages when the electronic structure is complicated (e.g., metallic) and the applicability of DFT-D3 is limited. Therefore, one can consider these two dispersion corrections not as competitors but as each other's supplement, and we suggest applying both methods in critical cases.

■ ASSOCIATED CONTENT

Supporting Information

Graphs of S66 and S22d sets with deviations from CCSD(T)/CBS reference to the D3/NL dispersion corrected and uncorrected functionals TPSS, TPSS0, B3LYP, and revPBE38. Tables of the center-of-mass and hydrogen bond distances of the S66 and S22d sets and estimated CCSD(T)/CBS equilibrium distances for the S22d set. Tables of dispersion uncorrected DFT distances for the water hexamer clusters, the three transition metal complexes, and molecules with intramolecular noncovalent interactions. This material is available free of charge via the Internet at http://pubs.acs.org/.

■ AUTHOR INFORMATION

Corresponding Author

*E-mail: grimme@thch.uni-bonn.de.

Notes

The authors declare no competing financial interest.

■ ACKNOWLEDGMENTS

This work was supported by the Deutsche Forschungsgemeinschaft within the framework of the SFB 858 ("Synergetic effects in chemistry: From additivity towards cooperativity.").

■ REFERENCES

(1) Stone, A. J. *The Theory of Intermolecular Forces*, 1st ed.; Oxford University Press: New York, 1997; Chapter 4, pp 50−63.
(2) Kaplan, I. G. *Intermolecular Interactions*, 1st ed.; J. Wiley & Sons: Chichester, England, 2006; Chapter 2, pp 44−50.
(3) Černý, J.; Hobza, P. *Phys. Chem. Chem. Phys.* **2007**, *9*, 5291.
(4) Grimme, S. *WIREs Comput. Mol. Sci.* **2011**, *1*, 211.
(5) Grimme, S.; Antony, J.; Ehrlich, S.; Krieg, H. *J. Chem. Phys.* **2010**, *132*, 154104.
(6) Zhao, Y.; Truhlar, D. G. *Acc. Chem. Res.* **2008**, *41*, 157−167.
(7) von Lilienfeld, O. A.; Tavernelli, I.; Röthlisberger, U.; Sebastiani, D. *Phys. Rev. Lett.* **2004**, *93*, 153004.
(8) Becke, A. D.; Johnson, E. R. *J. Chem. Phys.* **2005**, *123*, 154101.
(9) Sato, T.; Nakai, H. *J. Chem. Phys.* **2009**, *131*, 224104.
(10) Steinmann, S. N.; Corminboeuf, C. *J. Chem. Theory Comput.* **2010**, *6*, 1990−2001.
(11) Tkatchenko, A.; Scheffler, M. *Phys. Rev. Lett.* **2009**, *102*, 073005.
(12) Lee, K.; Murray, E. D.; Kong, L.; Lundqvist, B. I.; Langreth, D. C. *Phys. Rev. B* **2010**, *82*, 081101.
(13) Vydrov, O. A.; Van Voorhis, T. *J. Chem. Phys.* **2010**, *133*, 244103.
(14) Hujo, W.; Grimme, S. *Phys. Chem. Chem. Phys.* **2011**, *13*, 13942.
(15) Grimme, S.; Hujo, W.; Kirchner, B. *Phys. Chem. Chem. Phys.* **2012**, *14*, 4875.
(16) Vydrov, O. A.; Van Voorhis, T. *J. Chem. Theory Comput.* **2012**, *8*, 1929.
(17) Hujo, W.; Grimme, S. *J. Chem. Theory Comput.* **2011**, *7*, 3866.
(18) Grimme, S.; Ehrlich, S.; Goerigk, L. *J. Comput. Chem.* **2011**, *32*, 1456.
(19) Goerigk, L.; Kruse, H.; Grimme, S. *ChemPhysChem* **2011**, *12*, 3421−3433.
(20) Goerigk, L.; Grimme, S. *Phys. Chem. Chem. Phys.* **2011**, *13*, 6670.
(21) Burns, L. A.; Vazquez-Mayagoitia, A.; Sumpter, B. G.; Sherrill, C. D. *J. Chem. Phys.* **2011**, *134*, 084107.
(22) Jurecka, P.; Sponer, J.; Cerny, J.; Hobza, P. *Phys. Chem. Chem. Phys.* **2006**, *8*, 1985.
(23) Řezáč, J.; Riley, K. E.; Hobza, P. *J. Chem. Theory Comput.* **2011**, *7*, 2427.
(24) Gráfová, L.; Pitoňák, M.; Řezáč, J.; Hobza, P. *J. Chem. Theory Comput.* **2010**, *6*, 2365.
(25) Pérez, C.; Muckle, M. T.; Zaleski, D. P.; Seifert, N. A.; Temelso, B.; Shields, G. C.; Kisiel, Z.; Pate, B. H. *Science* **2012**, *336*, 897.
(26) Mitzel, N.; Losehand, U.; Wu, A.; Cremer, D.; Rankin, D. *J. Am. Chem. Soc.* **2000**, *122*, 4471.
(27) Cameron, T.; Deeth, R.; Dionne, I.; Du, H.; Jenkins, H.; Krossing, I.; Passmore, J.; Roobottom, H. *Inorg. Chem.* **2000**, *39*, 5614.
(28) Grimme, S. *Chem.—Eur. J.* **2004**, *10*, 3423.
(29) Mandel, G.; Donohue, J. *J. Acta Crystallogr.* **1972**, *B28*, 1313.
(30) Allen, F. H. *Acta Crystallogr.* **2002**, *B58*, 380 . Available under CSD-code HEXHEL.
(31) Shen, Y.; Chen, C.-F. *Chem. Rev.* **2012**, *112*, 1463.
(32) Ehrlich, S.; Moellmann, J.; Grimme, S. *Acc. Chem. Res.* **2012**, DOI: 10.1021/ar3000844.
(33) Mann, K. R.; Gordon, J. G.; Gray, H. B. *J. Am. Chem. Soc.* **1975**, *97*, 3553.
(34) Grimme, S.; Djukic, J.-P. *Inorg. Chem.* **2011**, *50*, 2619.
(35) Davis, H. B.; Einstein, F. W. B.; Glavina, P. G.; Jones, T.; Pomeroy, R. K.; Rushman, P. *Organometallics* **1989**, *8*, 1030.
(36) Grimme, S.; Djukic, J.-P. *Inorg. Chem.* **2010**, *49*, 2911.
(37) Schwabe, T.; Grimme, S.; Djukic, J.-P. *J. Am. Chem. Soc.* **2009**, *131*, 14156.
(38) Tao, J.; Perdew, J. P.; Staroverov, V. N.; Scuseria, G. E. *Phys. Rev. Lett.* **2003**, *91*, 146401.
(39) Grimme, S. *J. Phys. Chem. A* **2005**, *109*, 3067.
(40) Becke, A. D. *J. Chem. Phys.* **1993**, *98*, 5648.
(41) Stephens, P. J.; Devlin, F. J.; Chabalowski, C. F.; Frisch, M. J. *J. Phys. Chem.* **1994**, *98*, 11623.
(42) Zhang, Y.; Yang, W. *Phys. Rev. Lett.* **1998**, *80*, 890.
(43) Ernzerhof, M.; Scuseria, G. E. *J. Chem. Phys.* **1990**, *110*, 5029.
(44) Adamo, C.; Barone, V. *J. Chem. Phys.* **1999**, *110*, 6158.
(45) Johnson, E. R.; Becke, A. D. *J. Chem. Phys.* **2005**, *123*, 024101.
(46) Johnson, E. R.; Becke, A. D. *J. Chem. Phys.* **2006**, *124*, 174104.
(47) Grimme, S. *J. Comput. Chem.* **2006**, *27*, 1787.
(48) Ahlrichs, R. et al. TURBOMOLE, vers. 5.7; Universität Karlsruhe: Karlsruhe, Germany, 2005.
(49) Eichkorn, K.; Weigend, F.; Treutler, O.; Ahlrichs, R. *Theor. Chem. Acc.* **1997**, *97*, 119.
(50) Weigend, F. *Phys. Chem. Chem. Phys.* **2006**, *8*, 1057.
(51) Weigend, F.; Ahlrichs, R. *Phys. Chem. Chem. Phys.* **2005**, *7*, 3297.
(52) Goerigk, L.; Grimme, S. *J. Chem. Theory Comput.* **2011**, *7*, 291.
(53) Schäfer, A.; Huber, C.; Ahlrichs, R. *J. Chem. Phys.* **1994**, *100*, 5829.
(54) Andrae, D.; Haeussermann, U.; Dolg, M.; Stoll, H.; Preuss, H. *Theor. Chim. Acta* **1990**, *77*, 123.
(55) Xantheas, S. S. *Chem. Phys.* **2000**, *258*, 225.
(56) Grimme, S. *J. Chem. Phys.* **2006**, *124*, 034108.
(57) Bonifaci, C.; Ceccon, A.; Gambaro, A.; Ganis, P.; Santi, S.; Valle, G.; Venzo, A. *Organometallics* **1993**, *12*, 4211.
(58) Koide, A. *J. Phys. B* **1976**, *9*, 3173.
(59) The structural optimization with revPBE-D3 of the isolated hexahelicene molecule in ref 32 was not fully converged. Therefore, the distances R1 = 317 pm, R2 = 443 pm, and R3 = 546 pm given in that work are incorrect. The correct isolated molecule values with revPBE-D3 are R1 = 309 pm, R2 = 419 pm, and R3 = 513 pm, which were computed in this work with the Turbomole program (see Computational Details).